Published in final edited form as:
Med Dosim. 2009 ; 34(2): 133–139. doi:10.1016/j.meddos.2008.07.003.

Intra- and Inter-Fraction Mediastinal Nodal Region Motion: Implications for Internal Target Volume Expansions

Jonathan G. Thomas[1], **Rojano Kashani**[1], **James M. Balter**[1], **Daniel Tatro**[1], **Feng-Ming Kong**[1], and **Charlie C. Pan**[1,2]

[1]Department of Radiation Oncology, University of Michigan, Ann Arbor, MI

Abstract

Purpose/Objective—The purpose of this study is to determine the intra- and inter-fraction motion of mediastinal lymph node regions.

Materials/Methods—Ten patients with non-small cell lung cancer underwent controlled inhale and exhale CT scans during two sessions (40 total data sets) and mediastinal nodal stations 1–8 [Chapet, et al, IJROBP 2005;63:170–8] were outlined. Corresponding CT scans from different sessions were registered to remove setup error and in this reference frame, the center-of-mass (COM) of each nodal station was compared for right-left (RL), anterior-posterior (AP), and superior-inferior (SI) displacement. In addition, an anisotropic volume expansion encompassing the change of the nodal region margins in all directions was used. Intra-fraction displacement was determined by comparing same session inhale-exhale scans. Inter-fraction reproducibility of nodal regions was determined by comparing the same respiratory phase scans between two sessions.

Results—Intra-fraction displacement of COM varied between nodal stations. All nodal regions moved posteriorly and superiorly with exhalation, and inferior nodal stations showed the most motion. Based on anisotropic expansion, nodal regions expanded mostly in the RL direction from inhale to exhale. The inter-patient variations in intra-fraction displacement were large compared to the displacements themselves. Moreover, there was substantial inter-fractional displacement (~5 mm).

Conclusions—Mediastinal lymph node regions clearly move during breathing. Additionally, deformation of nodal regions between inhale and exhale occurs. The degree of motion and deformation varies by station and by individual. This study indicates the potential advantage of characterizing individualized nodal region motion to safely maximize conformality of mediastinal nodal targets.

Keywords

mediastinal lymph node; intrafraction motion; interfraction motion; lung cancer

Introduction

In patients with non-small cell lung cancer (NSCLC), mediastinal lymph nodes would be targeted to receive radiation if there is radiologic or pathologic evidence of involvement, or if the patient is undergoing elective nodal irradiation (ENI), in which the entire mediastinum would be treated. This latter practice has been the subject of ongoing debate. ENI intends to

[2]Corresponding author to whom all correspondence and reprint requests should be directed, University Hospital, 1500 East Medical Center Drive, Room UHB2C490, Ann Arbor, MI 48109-0010, Tel: (734) 936-7810, Fax: (734) 763-7370, cpan@med.umich.edu.

Conflict of Interest Notification: No actual or potential conflicts of interest exist

irradiate lymph nodes to treat occult metastases, but studies of alternative treatments omitting ENI have shown post-RT recurrence rates as low as 0–7% in early stage NSCLC [1–3], raising questions about the usefulness of this practice. On the other hand, the true rate of regional involvement can be underestimated by the current radiologic and pathologic methods [4], and surgical series have shown the rate of occult metastases in stage 1 NSCLC to be as high as 26% [5,6]. Further compounding the difficulty in interpreting the studies, the role of incidental irradiation of lymph nodes is only recently being appreciated [7]. Despite the controversy about its necessity in elective cases, most agree that lymph node irradiation still has a role in the treatment of NSCLC, and as predictions of which nodal regions are at-risk for metastasis improve [8], these at-risk regions can be targeted to treat micrometastases.

Treatment of mediastinal lymph nodes and the regions in which they reside is complicated by the fact that they are moving targets. The limitation of enlarging the target volume to account for motion is increased irradiation of normal tissue which can result in comorbidities such as radiation pneumonitis or esophagitis. Numerous studies have shown that treating a larger target volume results in higher rates of toxicity [9–14]. Additionally, the increasing emphasis on dose escalation to enhance local control has further underscored the importance of limiting lymph node target volumes to the smallest possible size. Despite these demands for greater precision, the motion of mediastinal lymph node regions has not been well characterized. However, with knowledge of the intra-fraction and inter-fraction motion of these lymph nodes in each patient, individualized treatment plans could be developed. These individualized plans, compared to standard uniform expansions, should reduce dose to normal tissue while allowing for increased dose to the target and reducing the chance for regional nodal failure.

While the motion due to breathing of calcified lymph nodes has been described [15], characterizing the motion of lymph node regions may prove more practical and valuable, especially for ENI. Involved or at-risk lymph node regions are frequently the targets of radiotherapy, so knowledge of their motion is most clinically useful.

Discrepancies between the expected dose distribution based on the treatment plan and the actual dose distribution delivered to a patient can result from uncertainties such as setup errors and intra-treatment and inter-treatment physiologic motion of the target. The International Commission on Radiation Units and Measurements Report 62 suggests that the planning target volume (PTV) include a set-up margin (SM) and an internal margin (IM) [16]. The SM accounts for uncertainties in patient position and beam alignment. The IM compensates for expected intra-fraction and inter-fraction physiologic movements and variations in size, shape and position of the clinical target volume (CTV), yielding the internal target volume (ITV). Patient-specific data on IM will allow for individualized thoracic target expansions, as opposed to a standard 1.0–2.0 cm uniform radial expansion to PTV currently in use, both in the community and per recent RTOG protocols.

A previous study [17] attempted to determine what margin needed to be added to mediastinal lymph node CTVs to adequately cover the ITV, which was approximated by creating an encompassing nodal volume (ENV) covering all contours of a particular node in 3 to 6 co-registered CT scans. In the study of 22 nodes, a symmetric margin of 5 mm was determined to be adequate to account for node mobility. However, mediastinal nodal motion is not necessarily symmetric, may differ between nodal regions, and may differ significantly from patient-to-patient.

The purpose of this study is to create a guide for future optimization studies by determining the intra- and inter-fraction motion of mediastinal lymph nodes, and hence, the necessary expansion of CTV to ITV.

Materials and Methods

Ten patients over 18 years of age with NSCLC (+/− mediastinal lymphadenopathy) were included in this study. CT scans of the patients were obtained at different breathing phases using an active breathing control device (ABC) described by Dawson et al. [18]. Four scans were obtained in each session: two at inhale (75– 80% vital capacity), one at half the volume of inhale and one at exhale (functional residual capacity) at two different sessions approximately 2 weeks apart. In this IRB-approved retrospective study, a pair of exhale and inhale scans from each session was used, yielding 40 total data sets. All data sets were analyzed for intra-fraction motion from exhale to inhale, and exhale data sets were additionally analyzed for inter-fraction motion.

One medical student (J.G.T), under the supervision of the senior author (C.C.P), outlined the mediastinal nodal stations and gross tumor volumes in each of the 40 data sets. These mediastinal nodal stations represent 12 divisions of the volume of the mediastinum where lymph nodes reside (Figure 1 and Table 1) according to the Mountain and Dressler classification [19] and the CT-based atlas developed at the University of Michigan [20]. The nodal regions of interest were 1R (right) and 1L (left), 2R and 2L, 3A (anterior) and 3P (posterior), 4R and 4L, 5, 6, 7, and 8 (see Figure 2 and Figure 3). Additionally, 13 radiologically evident lymph nodes in patients with mediastinal lymphadenopathy were also outlined for comparison of individual lymph node motion with nodal station motion (Table 7).

Intra-fraction motion due to breathing was evaluated by measuring the movement of the centroid location of each nodal station from inhale to exhale in right-left (RL), anterior-posterior (AP), and superior-inferior (SI) directions. The intra-fraction mean and standard deviation (SD) in each direction are reported in Table 2. The morphologic change and deformability of each station due to breathing was analyzed by determining the asymmetric expansion of inhale volume needed to encompass the exhale volume, shown in Table 4a. The inferior expansion from exhale covering inhale was also measured.

Inter-fraction motion was evaluated by comparing same breathing state scans of the patient from two different sessions. To account for setup errors, the CT volumes were registered on the spine, using rigid body transformation allowing for translation and rotation only. In this reference frame, the nodal station centroids were then compared for right-left (RL), anterior-posterior (AP), and superior-inferior (SI) displacement. The inter-fraction mean, SD and absolute range of displacement in RL, AP and SI directions are reported in Table 3. The morphologic change and deformability of each station from one session to the next was analyzed by determining the asymmetric expansion of inhale volume needed to encompass the exhale volume (Table 6).

Results

Intra-fraction Motion

Displacement of the mediastinal nodal regions varied by station. As seen in Table 2, the mean inferior displacement of the nodal station centroids from exhale to inhale is more pronounced in the more inferior nodal stations as expected. For example, paraesophageal station 8 showed a mean inferior displacement of 13.2 mm (SD = 8.2 mm) compared with 2.8 mm (SD = 4.0) in retrotracheal station 3P. Of notable exception, in 5 of 10 patients,

station 1L and 1R moved superiorly upon inhalation, with mean displacements of −1.1 (SD = 3.3 mm) and −0.7 mm (SD= 2.9 mm) respectively. Generally, nodal station centroids moved posteriorly upon exhalation. The right-sided station centroids 1R, 2R, and 4R generally moved to the right upon exhalation, while left-sided station centroids 1L, 2L, and 4L generally moved to the left upon exhalation. The inter-patient variation in breathing movement was large compared to the range of movement, evidenced by the large standard deviations.

As seen in Table 4a, intra-fraction inhale-to-exhale volumes of all regions expanded anisotropically in all directions. All regions except 1L, 1R, 3A, and 3P expanded superiorly. In the exhale covering inhale expansion (Table 4b), all regions expanded inferiorly with increased magnitude in more inferior stations.

Intra-fraction tumor motion (Table 6) followed the same general pattern—centroid motion was anterior and inferior upon inhalation. The more inferior structures had larger inferior displacements upon inhalation. However, there was no consistent correlation between lung tumor motion and motion of nearby node regions. Additionally, though lymph nodes that were contoured generally moved similarly to the centroids of the nodal region in which they belonged (Table 7), it cannot be said that measurement of one approximates the other.

Inter-fraction Motion

Displacement of the nodal region centroid relative to the axial skeleton between sessions (inter-fraction) demonstrated large standard deviations in all nodal regions, as reported in Table 3 Standard deviation and maximum displacement were generally largest in the SI direction.

Inter-fraction exhale-to-exhale anisotropic volume expansion showed considerable variation in nodal station volume and shape between sessions, particularly in the more inferior stations. Among the inferior stations, station 7 (subcarinal) showed the least change in volume and shape. This volume is delineated tightly adjacent to the carina, which is a more fixed mediastinal structure.

Discussion

This study has shown that between inhale and exhale, mediastinal nodal regions move in all directions and change in size and shape, with the magnitude depending on the location within the mediastinum. There also are considerable inter-patient differences of magnitude of nodal region motion. Moreover, these regions are not stationary from one breath-hold session to the next and demonstrate significant inter-fraction movement.

The intra-fraction displacement of mediastinal nodal regions is due primarily to breathing, though other factors such as heartbeat can also affect motion [21,22]. The inferior displacement of the nodal stations during inhalation is consistent with a downward pull from a contracting diaphragm. The measured mean exhale-to-inhale inferior volume expansion for station 8 (19.6 mm, SD = 9.0 mm), whose lower border is the GE junction, is consistent with the excursions measured in studies of supine diaphragmatic motion under normal-breathing conditions [23].

The more inferior stations are most affected by the vertical pull of the diaphragm as expected. The most superior stations 1L and 1R, which in 5 of 9 patients (one patient by strict definition did not have these stations) show superior displacement and volume expansion on inhalation, may be pulled upward by the chest wall expansion or the contracting accessory respiratory muscles of the neck. The posterior displacement and

volume expansion on exhalation is uniform in all nodal stations, which is consistent with the mediastinal contents being pulled forward by the expanding chest wall during inspiration.

In concurrence with a study measuring displacement of 27 calcified lymph nodes via fluoroscopy[15], the amplitude of mediastinal lymph node motion is greatest in the craniocaudal axis and least in the mediolateral axis. However, for the dorsoventral axis they showed a mean displacement of 2.6 mm (SD = 2.6, range = 0–9 mm) which differed from the larger displacements in both lymph node and nodal station (table 2 and table 7) found in this study. The two studies also differ in that inhale scans were taken at 75–80% of vital capacity in this study, while the fluoroscopy study acquired measurements during “quiet respiration”, which is presumably farther from vital capacity. Furthermore, while the fluoroscopy study did not find a statistically significant difference between infracarinal and supracarinal node displacement, this study found a trend of superior-to-inferior increasing magnitude of displacement of nodal region centroids. However, these two studies cannot be directly compared since the fluoroscopy studied calcified nodes, not nodal regions, and 13 of the 27 nodes were hilar, and hilar regions were not examined in this study.

The marked lateral volume expansion from inhale to exhale demonstrates the deformability of the mediastinum. When pulled more taut by the inferior force of the diaphragm and the anterior force of the chest wall, as well as pushed in by the expanding lungs, the mediastinum tends to shrink medially. Upon exhalation, the deformable mediastinum can relax and its right and left margins expand laterally.

The degree of motion varies substantially, depending on the individual and the nodal station. Because breathing mechanics (i.e., use of accessory muscles versus diaphragm), size, and lung compliance varies from person to person, the large variance between persons in intra-fraction motion was expected. The lack of inter-fraction reproducibility relative to the axial skeleton indicates that the regions of the mediastinum where lymph nodes lie are not firmly fixed to adjacent structures. Station 8 demonstrated the least vertical direction reproducibility, which again suggests that this region of the mediastinum is more mobile than the other regions which are more closely adherent to the trachea, main bronchi, and great vessels. This lack of inter-fraction reproducibility also suggests that patients may benefit from daily imaging and/or localization of the mediastinal regions if they are to be treated.

With respect to tumor motion (table 6), consistent with other studies [21,22], amplitude was greatest in the cranio-caudal direction, especially in the case of lower lobe tumors. The tumors also moved anteriorly on inhalation, similar to the lymph node regions. Right-left motion was less predictable and less reproducible between sessions. However, this study was limited as it was not the focus of this investigation.

This investigation suggests, in agreement with previous studies of motion of lung tumors and calcified mediastinal lymph nodes [15,21], that the target motion is variable between patients, and a generalized, population-based expansion to create the PTV may either overcompensate or undercompensate for each individual’s targets. Instead, an individualized expansion based on each patient’s own breathing characteristics is needed for a reduced PTV. This necessitates the use of technology that can image the individual’s breathing motion pattern. The current study used active breathing control to determine an individual’s target position variations, but in practice, 4D datasets would offer several advantages over ABC in this function. It would allow measurement of not only full inhale and exhale, but also the intermediate points in the breathing cycle. It would also better characterize the path of motion, hysteresis and how much time the target spends at each segment of the path.

These factors can all be used to tailor the PTV to the target. In this study, ABC was used as a surrogate technique to approximate the nodal region motion in normal breathing.

One limitation of this study is that, with the notable exception of ENI, it is often involved discrete lymph nodes, not lymph node regions, which are targeted. In this study, radiographically evident lymph nodes moved analogously to the regions to which they belonged, but further studies are needed to characterize whether the motions are more congruous in certain patients, or whether lymph node size or fixation plays a role.

The variable thoracic anatomy makes it difficult to draw generalized conclusions about nodal regions. For example, the border between stations 1L and 1R stations 2L and 2R is defined as the plane in which the left brachiocephalic vein crosses the trachea. However, due to variable anatomy, one patient by definition did not have station 1L and 1R, and another patient did not have station 2L and 2R. This variability prompted another study to combine stations 1 and 2 [20]. The size and shape of each region is unique in each person. This further highlights the need for individualized, rather than generalized, expansions.

Despite better characterization of the motion of each lymph node region, due to significant inter-patient variability and the small population of this study, a generalized PTV expansion for each region that can be applied to the whole population cannot be recommended. This study predicts that characterization of lymph node region motion for each individual that allow individualized target expansions can result in increased dose to target and decreased dose to normal tissue, but future dosimetric studies are necessary to confirm this. While ABC allows for both motion characterization and immobilization of target for treatment, patients may have difficulty tolerating it. With the advent of 4D datasets, data for individualized motion characterization can be collected more quickly and practically and allow for individual expansion that, in combination with daily imaging and/or adaptive techniques, can safely maximize conformality of nodal targets.

Acknowledgments

Work supported in part by NIH P01-CA59827.

References

1. Rosenzweig KE, et al. Elective nodal irradiation in the treatment of non-small-cell lung cancer with three-dimensional conformal radiation therapy. Int J Radiat Oncol Biol Phys 2001;50(3):681–685. [PubMed: 11395236]
2. Emami B, et al. The impact of regional nodal radiotherapy (dose/volume) on regional progression and survival in unresectable non-small cell lung cancer: an analysis of RTOG data. Lung Cancer 2003;41(2):207–214. [PubMed: 12871784]
3. Senan S, et al. Can elective nodal irradiation be omitted in stage III non-small-cell lung cancer? Analysis of recurrences in a phase II study of induction chemotherapy and involved-field radiotherapy. Int J Radiat Oncol Biol Phys 2002;54(4):999–1006. [PubMed: 12419425]
4. Chang DT, Zlotecki RA, Olivier KR. Re-examining the role of elective nodal irradiation: finding ways to maximize the therapeutic ratio. Am J Clin Oncol 2005;28(6):597–602. [PubMed: 16317271]
5. Jeremic B. Incidental irradiation of nodal regions at risk during limited-field radiotherapy (RT) in dose-escalation studies in nonsmall cell lung cancer (NSCLC). Enough to convert no-elective into elective nodal irradiation (ENI)? Radiother Oncol 2004;71(2):123–125. [PubMed: 15110444]
6. Ginsberg RJ, Rubinstein LV. Randomized trial of lobectomy versus limited resection for T1 N0 non-small cell lung cancer. Lung Cancer Study Group. Ann Thorac Surg 1995;60(3):615–622. discussion 622-3. [PubMed: 7677489]

7. Chen M, et al. Long-term results of high-dose conformal radiotherapy for patients with medically inoperable T1-3N0 non-small-cell lung cancer: Is low incidence of regional failure due to incidental nodal irradiation? Int J Radiat Oncol Biol Phys 2006;64(1):120–126. [PubMed: 16198503]
8. Giraud P, et al. Probability of mediastinal involvement in non-small-cell lung cancer: a statistical definition of the clinical target volume for 3-dimensional conformal radiotherapy? Int J Radiat Oncol Biol Phys 2006;64(1):127–135. [PubMed: 16226394]
9. Graham MV, et al. Clinical dose-volume histogram analysis for pneumonitis after 3D treatment for non-small cell lung cancer (NSCLC). Int J Radiat Oncol Biol Phys 1999;45(2):323–329. [PubMed: 10487552]
10. Yorke ED, et al. Dose-volume factors contributing to the incidence of radiation pneumonitis in non-small-cell lung cancer patients treated with three-dimensional conformal radiation therapy. Int J Radiat Oncol Biol Phys 2002;54(2):329–339. [PubMed: 12243805]
11. Rancati T, et al. Factors predicting radiation pneumonitis in lung cancer patients: a retrospective study. Radiother Oncol 2003;67(3):275–283. [PubMed: 12865175]
12. Jenkins P, et al. Radiation pneumonitis following treatment of non-small-cell lung cancer with continuous hyperfractionated accelerated radiotherapy (CHART). Int J Radiat Oncol Biol Phys 2003;56(2):360–366. [PubMed: 12738310]
13. Tsujino K, et al. Predictive value of dose-volume histogram parameters for predicting radiation pneumonitis after concurrent chemoradiation for lung cancer. Int J Radiat Oncol Biol Phys 2003;55(1):110–115. [PubMed: 12504042]
14. Seppenwoolde Y, et al. Comparing different NTCP models that predict the incidence of radiation pneumonitis. Normal tissue complication probability. Int J Radiat Oncol Biol Phys 2003;55(3): 724–735. [PubMed: 12573760]
15. Jenkins P, Salmon C, Mannion C. Analysis of the movement of calcified lymph nodes during breathing. Int J Radiat Oncol Biol Phys 2005;61(2):329–334. [PubMed: 15667950]
16. Wambersie, A.; Landberg, T. Report 62. Prescribing, recording, and reporting photon beam therapy (Supplement to ICRU report 50). Washington, D.C.: International Commission on Radiation Units and Measurements; 1999.
17. van Sornsen de Koste JR, et al. What margins are necessary for incorporating mediastinal nodal mobility into involved-field radiotherapy for lung cancer? Int J Radiat Oncol Biol Phys 2002;53(5):1211–1215. [PubMed: 12128122]
18. Dawson LA, et al. The reproducibility of organ position using active breathing control (ABC) during liver radiotherapy. Int J Radiat Oncol Biol Phys 2001;51(5):1410–1421. [PubMed: 11728702]
19. Mountain CF, Dresler CM. Regional lymph node classification for lung cancer staging. Chest 1997;111(6):1718–1723. [PubMed: 9187199]
20. Chapet O, et al. CT-based definition of thoracic lymph node stations: an atlas from the University of Michigan. Int J Radiat Oncol Biol Phys 2005;63(1):170–178. [PubMed: 16111586]
21. Ekberg L, et al. What margins should be added to the clinical target volume in radiotherapy treatment planning for lung cancer? Radiother Oncol 1998;48(1):71–77. [PubMed: 9756174]
22. Seppenwoolde Y, et al. Precise and real-time measurement of 3D tumor motion in lung due to breathing and heartbeat, measured during radiotherapy. Int J Radiat Oncol Biol Phys 2002;53(4): 822–834. [PubMed: 12095547]
23. Langen KM, Jones DT. Organ motion and its management. Int J Radiat Oncol Biol Phys 2001;50(1):265–278. [PubMed: 11316572]

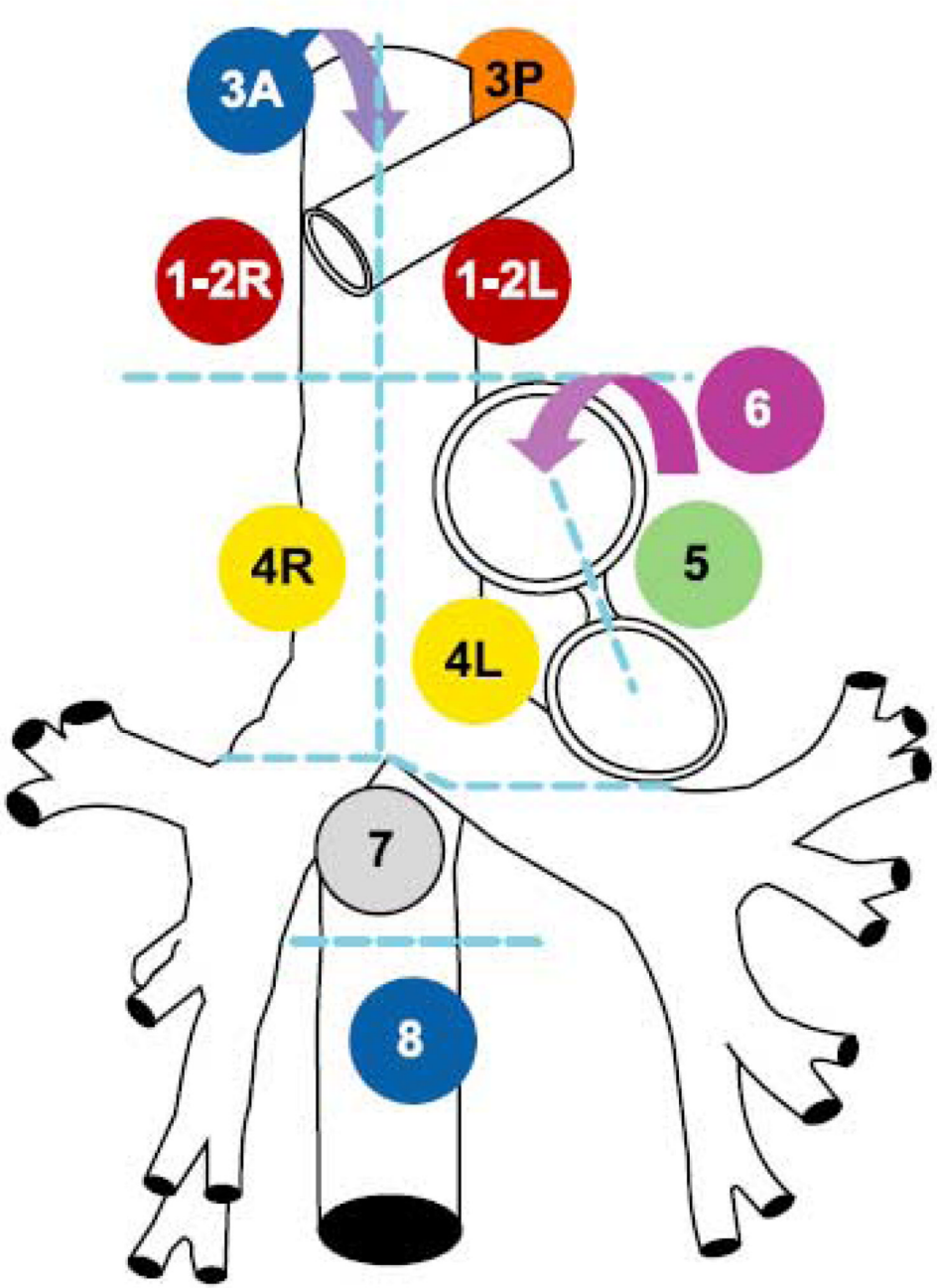

Figure 1.
Schema of Mountain and Dresler classification system [19]. Station 3A is anterior to Stations 1–2R and L and Stations 4R and L (blue arrow). Station 3P is posterior to trachea. Station 6 is anterior and lateral to aortic arch and ascending aorta (purple arrow).

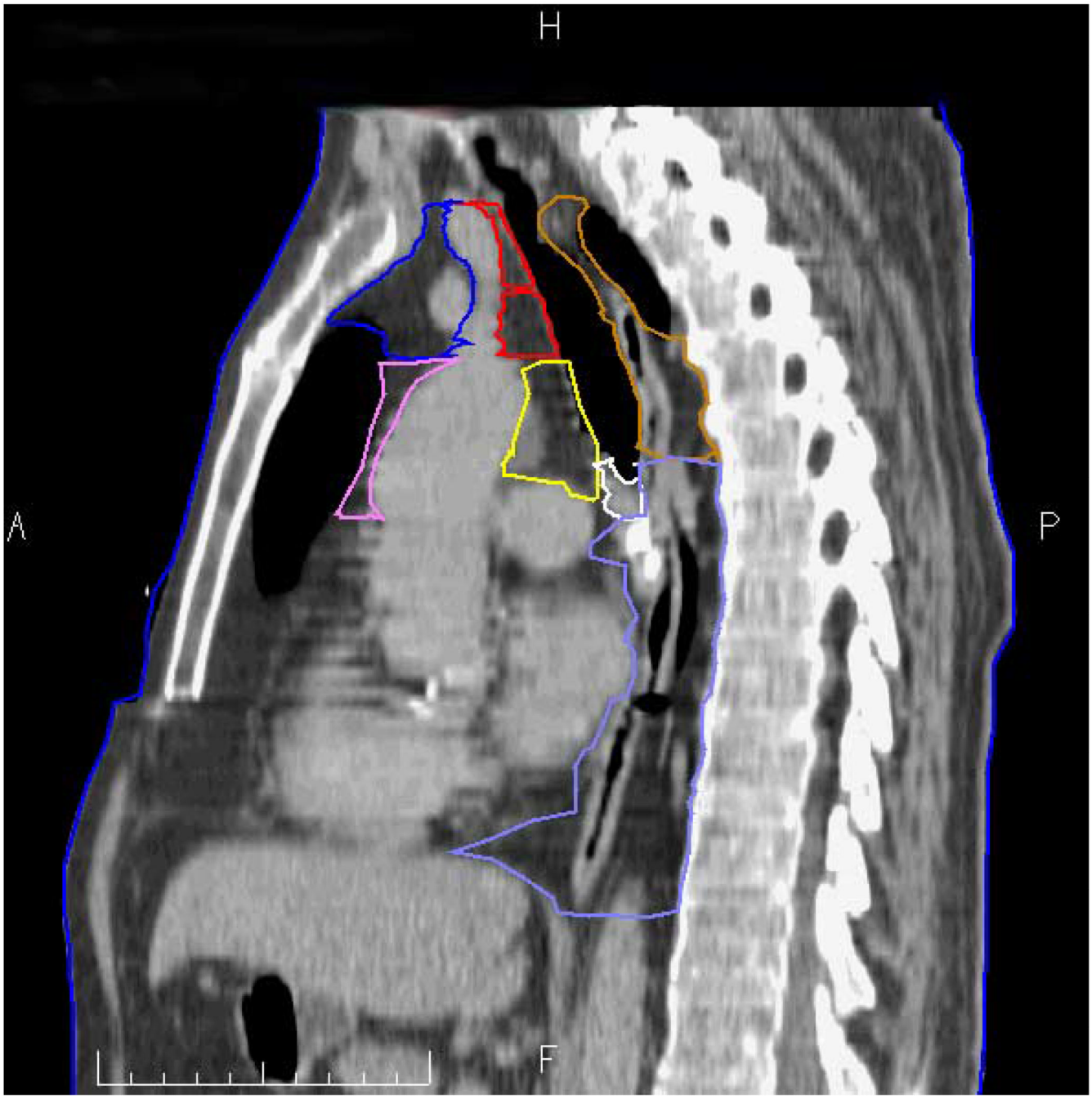

Figure 2.
Actual sagittal CT taken just right of midline. Station 1R and 2R = red; station 3A = blue; station 3P = brown; station 4R = yellow; station 6 = violet; station 7 = white; and station 8 = light blue. A = anterior, P = posterior, H= cranial, F = caudal.

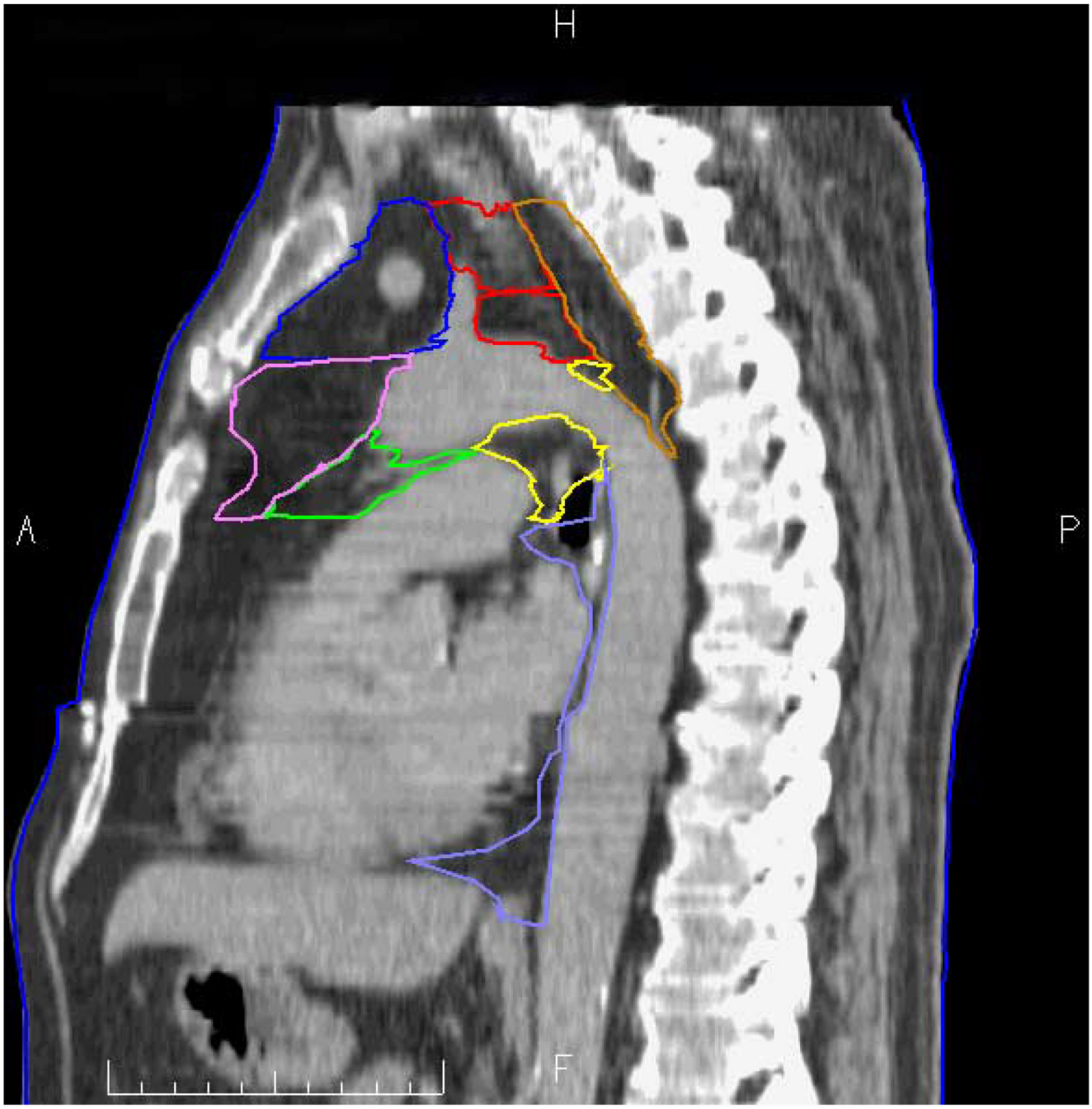

Figure 3.
Actual sagittal CT taken just left of midline. Station 1L and 2L = red; station 3A = blue; station 3P = brown; station 4L = yellow; station 5 = green; station 6 = violet; station 7 = white; and station 8 = light blue. A = anterior, P = posterior, H= cranial, F = caudal.

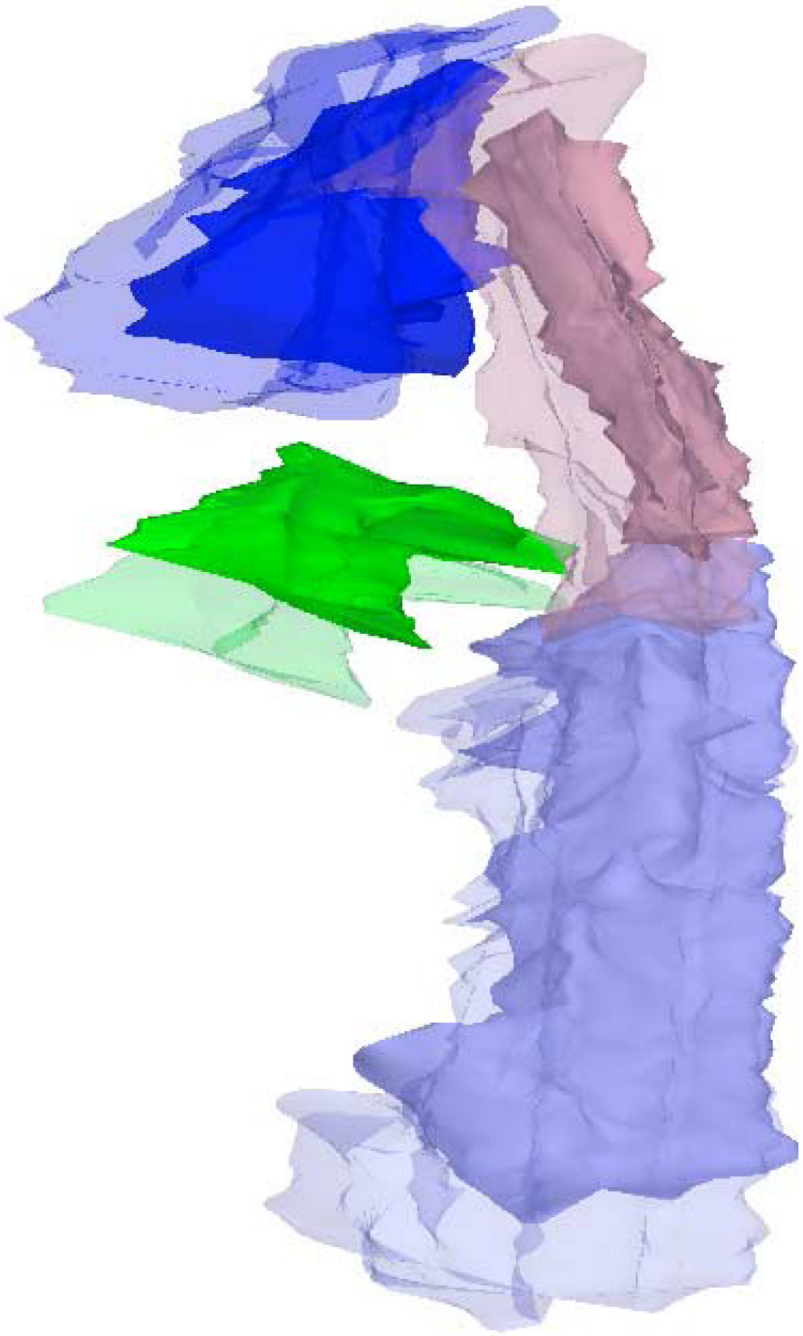

Figure 4.
Reconstructed 3D image comparing exhale (solid) and inhale (translucent) volumes. Station 3A = blue; station 3P = brown; station 5 = green; and station 8 = light blue.

Table 1

Station number and location

Station number	Location
1L	Left highest mediastinal
1R	Right highest mediastinal
2L	Left upper paratracheal
2R	Right upper paratracheal
3A	Pre-vascular
3P	Retrotracheal
4L	Left lower paratracheal
4R	Right lower paratracheal
5	Subaortic
6	Para-aortic
7	Subcarinal
8	Paraesophageal (below carina)

Table 2

Mean Intra-Fraction Displacement of Nodal Region centroid (Inhale to Exhale), in mm, with range and SD. Left, Posterior, and Superior are positive. RL= Right-Left; AP = Anterior-Posterior; SI = Superior-Inferior.

Nodal Station	RL			AP			SI		
	Mean	Range	SD	Mean	Range	SD	Mean	Range	SD
1L	0.2	−5.8--5.0	2.4	6.1	−1.1—19.1	5.2	−1.1	−10.1—3.4	3.3
1R	−1.2	−5.3—2.5	2.1	4.9	−0.7—17.3	4.7	−0.7	−7.3—3.4	2.9
2L	0.1	−7.1—6.7	3.5	9.2	−0.4—25.0	7.1	3.4	−2.3—12.3	3.5
2R	−2.1	−6.9—2.9	2.6	8.3	−6.2—23.6	6.9	3.8	−2.1—13.7	3.7
3A	1.8	5.3—7.2	3.3	7.3	−1.1—21.1	7.0	0.3	−6.6—6.3	3.2
3P	−0.2	−5.3—3.8	2.3	4.0	−0.8—11.0	3.0	2.8	−9.7—7.1	4.0
4L	0.6	−5.1—5.9	2.5	8.2	−0.2—17.8	4.9	8.8	−0.2—15.8	3.8
4R	−1.2	−7.1—3.1	3.1	9.7	0.9—21.6	5.2	8.9	−0.2—16.2	4.7
5	2.4	−1.6—9.1	2.6	8.2	−4.2—20.9	5.7	8.1	1.9—14.4	3.2
6	0.3	−7.2—7.3	4.3	9.2	1.0—22.2	6.4	7.6	−0.3—16.2	4.7
7	−0.9	−5.6—2.7	2.4	8.3	0.2—18.5	4.9	10.8	0.1—19.0	5.0
8	0.9	−3.3—4.7	2.4	7.3	−1.3—15.3	3.8	13.2	0.8—25.6	8.2

Table 3

Mean Inter-Fraction Displacement of Nodal Region centroid (measured on Exhale scans from two different sessions), in mm with absolute value minimum-absolute value maximum and SD. Left, Posterior, and Superior are positive

Nodal Station	RL			AP			SI		
	Mean	Range	SD	Mean	Range	SD	Mean	Range	SD
1L	0.5	0.1–5.0	2.8	0.2	0.0–4.2	2.3	−0.2	1.2–9.6	5.0
1R	0.7	0.2–6.8	3.3	−1.6	1.2–4.6	2.9	−0.4	0.6–10.9	5.6
2L	2.0	0.5–9.5	4.5	1.9	0.5–5.7	3.4	0.4	0.2–8.8	5.4
2R	0.6	0.4–6.4	3.4	0.4	0.3–6.7	3.8	0.5	0.3–9.7	5.7
3A	−1.0	0.5–9.0	3.7	−1.6	0.1–5.8	3.3	−0.9	0.1–8.2	3.4
3P	0.6	0.3–6.2	2.5	0.4	0.0–5.8	2.4	−1.1	0.2–7.5	4.2
4L	−0.1	0.1–3.7	2.1	0.0	0.2–5.9	2.7	1.3	0.5–7.3	4.6
4R	1.0	0.3–6.5	3.0	−1.3	0.1–9.5	4.5	1.3	0.7–8.9	6.0
5	−0.4	1.1–5.8	3.9	−0.6	0.4–7.8	3.4	−0.4	0.2–5.1	3.4
6	−0.4	0.1–6.2	3.0	−2.0	1.4–6.6	3.6	−0.1	1.9–5.5	3.5
7	−0.1	0.1–3.2	1.7	−0.3	0.1–7.1	3.3	−0.6	0.9–7.6	5.0
8	0.3	0.1–5.1	2.1	0.0	0.7–4.5	2.8	−0.7	1.2–22.9	11.2

Table 4

Table 4a:

Mean and SD of intra-fraction anisotropic volume expansion of inhale to cover exhale, in mm

Nodal Station	Right expansion		Left expansion		Anterior expansion		Posterior expansion		Inferior expansion		Superior expansion	
	Mean	SD	Mean	SD	Mean	SD	Mean	SD	Mean	SD	Mean	SD
1L	5.9	4.3	7.6	4.8	3.1	6.2	10.0	5.9	1.1	2.7	0.2	0.9
1R	7.8	4.2	4.8	2.9	2.7	3.4	10.3	9.3	0.9	2.3	0	0
2L	6.0	4.1	6.2	4.3	0.6	1.8	13.1	8.6	0.3	1.2	3.8	4.3
2R	7.6	5.0	3.0	3.2	1.1	2.8	11.9	8.1	0.3	1.2	3.6	4.2
3A	10.3	7.5	13.6	9.4	3.9	6.5	15.4	8.9	0.2	1.1	0	0
3P	13.1	5.9	13.8	6.0	1.1	1.8	9.1	4.5	0	0	0	0
4L	5.8	4.7	18.2	7.5	3.6	5.4	17.7	9.0	0	0	7.7	4.6
4R	15.9	7.8	5.1	4.6	1.0	2.8	18.6	6.4	0	0	7.5	5.1
5	11.5	5.5	13.3	6.4	6.3	7.8	16.8	9.5	0	0	7.3	4.0
6	22.1	11.6	12.5	6.6	7.4	9.6	22.5	9.2	0	0	8.9	5.1
7	10.3	3.6	11.1	4.4	0.3	1.2	13.1	5.9	0	0	13.6	7.6
8	21.2	9.1	20.9	8.6	19.3	8.3	10.4	5.3	0	0	12.4	6.5

Table 4b:

Mean and SD of intra-fraction anisotropic volume expansion of exhale to cover inhale, in mm

Nodal Station	Inferior Expansion	
	Mean	SD
1L	3.8	3.9
1R	3.8	3.9
2L	6.8	4.7
2R	6.7	4.7
3A	7.7	3.7
3P	10.6	6.3
4L	13.8	4.2
4R	14.6	8.3

Table 4b:

Mean and SD of intra-fraction anisotropic volume expansion of exhale to cover inhale, in mm

Nodal Station	Inferior Expansion	
	Mean	SD
5	10.8	4.3
6	10.2	4.0
7	13.8	5.2
8	19.6	9.0

Table 5

Mean and SD of inter-fraction anisotropic volume expansion of 1st session exhale to cover 2nd session exhale, in mm

Station	Right expansion		Left expansion		Anterior expansion		Posterior expansion		Inferior expansion		Superior expansion	
	Mean	SD	Mean	SD	Mean	SD	Mean	SD	Mean	SD	Mean	SD
1L	3.9	3.0	5.9	6.3	3.7	2.5	2.6	2.7	2.9	4.9	3.4	3.0
1R	4.1	3.8	2.4	2.6	3.4	4.1	2.4	2.5	2.9	4.9	4.1	4.0
2L	3.9	4.8	6.2	5.2	9.1	5.2	2.1	2.3	5.0	5.6	3.3	3.6
2R	4.2	4.1	2.6	2.7	4.7	3.5	1.8	3.6	4.2	5.4	3.4	3.9
3A	4.9	3.6	6.1	3.8	7.3	6.0	11.6	5.5	3.4	3.7	3.1	3.0
3P	8.7	6.0	8.4	7.5	5.3	4.0	3.3	2.4	3.8	3.9	2.6	3.1
4L	4.7	3.7	12.2	8.4	11.3	8.7	11.8	8.0	3.4	2.8	2.1	2.8
4R	9.6	7.5	5.8	3.3	7.0	6.1	8.0	5.4	5.7	6.4	2.4	2.7
5	7.2	5.1	9.2	5.8	7.3	6.7	20.5	11.4	3.1	4.0	1.5	2.5
6	14.0	13.3	9.0	7.2	9.5	9.6	19.6	9.7	2.9	3.8	1.1	1.9
7	3.9	2.5	4.6	4.2	4.7	5.0	1.8	2.0	3.9	3.1	0.7	2.2
8	12.4	6.4	11.9	6.8	14.9	7.1	5.3	6.3	4.3	6.9	1.4	2.3

Table 6

Tumor location and intra-fraction centroid displacement (Inhale to Exhale) in mm. Left, Posterior, and Superior are positive

	1st session displacement				2nd session displacement		
Tumor Location	RL	AP	SI		RL	AP	SI
Rt lower lobe	3.4	−1.3	2.1		−3.3	−0.2	−2.3
Rt lower lobe	3.2	10.2	25.1		2.0	5.8	21.6
Rt lower lobe	4.9	7.8	20.6		3.6	7.3	22.0
Rt lower lobe	7.0	16.0	15.0		7.3	13.4	20.3
Rt upper lobe	1.6	7.4	2.8		−1.0	2.9	−0.1
Rt upper lobe	6.7	8.2	5.4		10.1	8.5	7.6
Rt upper lobe	1.3	5.8	0.7		1.7	4.3	−1.3
Lft lower lobe	−3.4	3.9	−21.1		−10.5	7.9	28.2
Lft upper lobe	−0.1	0.1	6.2		−0.6	2.9	3.8
Lft upper lobe	−1.4	2.9	3.4		2.3	−1.0	3.6

Table 7

Lymph node intra-fraction (Inhale to Exhale) and inter-fraction (Exhale to Exhale) centroid displacement in mm. Left, Posterior, and Superior are positive

	1st session Intra-fraction				2nd session Intra-fraction				Inter-fraction		
Lymph node location	**RL**	**AP**	**SI**		**RL**	**AP**	**SI**		**RL**	**AP**	**SI**
4L	1.6	6.1	9.2						3.8	12.9	37.3
5	1.0	7.8	5.7						0	−3.1	−3.6
5	3.6	5.9	9.6		5.5	12.9	10.9		−.7	−6.1	−5.6
5	6.6	5.4	7.6		4.5	7.1	13.0		−1.4	−2.6	−6.9
5	7.8	6.1	8.0		5.6	6.6	12.1		−0.1	−3.2	−8.7
4L	−3.7	−0.6	5.4						0.2	−1.6	−1.9
3P	−4.7	2.6	−1.4						5.3	−3.7	0
1R	−2.1	10.7	11.2		−0.6	7.0	3.0		−2.0	3.2	9.4
2R	−6.6	21.6	12.4		−1.9	9.8	1.9		−6.4	7.9	7.9
4R	−3.4	19.9	17.0		0	8.2	8.2		−3.3	6.3	9.3
4L	0.5	12.3	12.8		0.5	7.1	8.0		−0.1	3.1	4.7
8	−3.1	21.4	17.2		−2.5	10.6	8.1		−2.0	6.7	8.9
3P	−1.3	−4.6	0.3		−0.3	−0.7	0		2.8	−4.0	1.9